Structural and electronic properties of $ZnGeAs_2$

A. Janotti, Su-Huai Wei, S. B. Zhang, and Sarah Kurtz
National Renewable Energy Laboratory, Golden, Colorado 80401
(Received 25 October 2000; published 1 May 2001)

Using a first-principles band-structure method based on density functional theory, we have studied the structural and electronic properties of $ZnGeAs_2$. In agreement with experimental data, $ZnGeAs_2$ is found to be nearly lattice matched to its binary analog GaAs. The calculated band structures show that $ZnGeAs_2$ in the chalcopyrite structure has a direct band gap, about 0.31 eV smaller than the band gap of GaAs. The calculated valence-band offset between $ZnGeAs_2$ and GaAs is 0.18 eV; thus, the band alignment of the $ZnGeAs_2$/GaAs system is type I, with both holes and electrons localized on $ZnGeAs_2$. We also find that at low temperature, $(ZnGeAs_2)_{0.5}(GaAs)$ forms a stable stannite structure. However, the band gap and the mixing energy of the alloy at higher temperature depend sensitively on the local short-range order. The calculated formation energies of the $(ZnGeAs_2)_n(GaAs)_{2n}$ superlattices along the [001] direction show strong nonmonotonic behavior, with the formation energy ΔH_n maximized at $n=2$. We compared our results for the $ZnGeAs_2$/GaAs system to the well-studied $CuGaSe_2$/ZnSe system. The differences between these two systems are explained in terms of their ionicity and their relative strength of the anion *p* and cation *d* couplings.

DOI: 10.1103/PhysRevB.63.195210 PACS number(s): 71.15.Ap, 73.40.−c

I. INTRODUCTION

Ternary semiconductors that crystallize in a chalcopyrite structure form a group of important semiconductor compounds with diverse structural, optical, and electronic properties.[1] Going from zinc-blende binary semiconductor compounds (e.g., GaAs and ZnSe) to their ternary analogs (e.g., $ZnGeAs_2$ and $CuGaSe_2$) in a chalcopyrite structure greatly enlarges the range and choice of materials with optimized electronic and optical properties for device applications. One example is $ZnGeAs_2$, which is the ternary analog of the binary compound GaAs (in the sense that the average of $\langle ZnGe \rangle$ is Ga).[2] Because of the noncubic character of the chalcopyrite structure, the degeneracy at the top of the valence band is removed, thus making it suitable for high-efficiency sources of spin-polarized photoelectrons.[3,4] Its large nonlinear optical coefficients also make it suitable for nonlinear optical applications.[1] Because $ZnGeAs_2$ and GaAs have a good lattice match and $ZnGeAs_2$ has a direct band gap of about 1.15 eV at room temperature, $ZnGeAs_2$ has also been considered a good candidate material for high-efficiency multijunction solar cells.[5] However, in spite of the importance of $ZnGeAs_2$ in optoelectronic applications, very little is known about its physical properties. For example, early experimental measurements[6,7] found that $ZnGeAs_2$ has a band gap around 0.8 eV, whereas more recent data[8] show that $ZnGeAs_2$ has a direct band gap of 1.15 eV at room temperature. Also unclear is the sign of $\delta u = u - \frac{1}{4}$ for $ZnGeAs_2$, where u is the anion displacement parameter for the chalcopyrite compound. The value $\delta u = 0.014$, derived by Jaffe and Zunger[2] from Pauling's ionic radii,[9] is fairly large and positive. However, experimental measurements[10,11] suggest that δu is close to zero. Furthermore, no study has been done on the electronic structures and stabilities of $(ZnGeAs_2)_{1-x}(GaAs)_{2x}$ alloys and $ZnGeAs_2$/GaAs interfaces. Understanding these properties are important for future electronic device applications involving these materials.

In this paper, we provide a systematic study of the electronic and structural properties of $ZnGeAs_2$/GaAs systems through first-principles band-structure calculations. We calculated the (i) structural parameters and bulk modulus of chalcopyrite $ZnGeAs_2$, (ii) electronic band structure of $ZnGeAs_2$, (iii) long-range and short-range order/disorder-induced band-gap reduction in $ZnGeAs_2$, (iv) formation energy and band-gap bowing of $(ZnGeAs_2)_{1-x}(GaAs)_{2x}$ alloys at $x=0.5$, (v) band alignment at the $ZnGeAs_2$/GaAs interface, and (vi) formation energies of the $(ZnGeAs_2)_n(GaAs)_{2n}$ superlattices as a function of layer thickness n. We provide the following results: (a) in agreement with experimental data,[12] $ZnGeAs_2$ is nearly lattice matched to its binary analog GaAs; (b) $ZnGeAs_2$ in the chalcopyrite structure has a direct band gap, about 0.31 eV smaller than the band gap of GaAs; (c) at $x=0.5$, the $(ZnGeAs_2)_{1-x}(GaAs)_{2x}$ alloy forms a stable stannite structure [ZnAs/GaAs/GeAs/GaAs superlattice along the (201) direction]: however, the band gap of the alloy is very sensitive to the long- or short-range order in the alloy; (d) the calculated valence-band offset and conduction-band offset between $ZnGeAs_2$ and GaAs are 0.18 eV and 0.13 eV, respectively, with both holes and electrons localized on $ZnGeAs_2$ (i.e., the alignment is type I); (e) the formation energies of the $(ZnGeAs_2)_n(GaAs)_{2n}$ superlattice change nonmonotonically, with minima at $n=1$ and $n=\infty$ and a maximum at $n=2$, indicating that it could be difficult to form a sharp $ZnGeAs_2$/GaAs interface. Our calculated results for the $ZnGeAs_2$/GaAs system are compared with the $CuGaSe_2$/ZnSe system.[13–15] We show that relative to the $CuGaSe_2$/ZnSe system, the band-gap reduction and the valence-band offset between $ZnGeAs_2$ and GaAs are small. The differences between $ZnGeAs_2$/GaAs and $CuGaSe_2$/ZnSe are explained in terms of the relative strength of the *p-d* coupling in these two systems.[15] In the following, we describe our calculation methods and discuss our calculated results.

II. METHOD OF CALCULATIONS

The tetragonal chalcopyrite structure of $ZnGeAs_2$ (space group $I\bar{4}2d$-D_{2d}^{12}) can be considered as derived from the cubic zinc-blende structure of GaAs (space group $F\bar{4}3m$-T_d^2) by converting every Ga+Ga pair into a Zn+Ge pair. In the chalcopyrite structure, the Zn and Ge atoms form a $(Zn)_2/(Ge)_2$ superlattice along the [201] direction in one of the face-centered-cubic (fcc) sublattices. Each Zn or Ge atom is surrounded by four As atoms, and each As atom is surrounded by two Zn and two Ge atoms. The As atom is shifted from the center of the Zn_2Ge_2 tetrahedron, which causes the Zn-As and Ge-As bond lengths to be different. The chalcopyrite structure is described by two external parameters, a (the lattice parameter in the x-y plane) and c (the lattice parameter perpendicular to the x-y plane), and by one internal parameter u, which is related to the displacement of the anion in the x direction. To calculate these structural parameters, we used the following procedure:[16] we first determined the values of $(c/a)(V)$ and $u(V)$ that minimize the total energy E for a given V. We then fitted the $E(V)$ curve to Murnaghan's equation of states to obtain $V_{\rm eq}$, $(c/a)_{\rm eq}$, $u_{\rm eq}$, and the bulk modulus.

The band-structure and total-energy calculations were performed using density functional formalism within the local density approximation (LDA),[17] as implemented by the general potential, all electron, linearized augmented plane-wave (LAPW) method.[18] The Zn, Ga, and Ge $3d$ electrons were treated in the same footing as the other valence electrons. For all the atoms, we used the muffin-tin radius of $R_{\rm MT}=2.2$ a.u. No shape approximation was used for either the potential or the charge density. We used the Ceperley-Alder[19] exchange correlation potential as parametrized by Perdew and Zunger.[20] The Brillouin zone integration was performed using the ten special Monkhorst-Pack[21] k points for the zinc-blende structure and their equivalent k points[22] for the superstructures.

It is well known that although the LDA is good for calculating ground-state properties, it underestimates the band gap of semiconductors. To correct this band-gap error, we adopted a simple procedure[16,23] as follows: we added to the LDA potential an atom-dependent, spherical, and repulsive potential inside the muffin-tin spheres centered at each atomic and interstitial sites α with

$$V^{\alpha}=\bar{V}^{\alpha}+V_0^{\alpha}\left(\frac{r_0^{\alpha}}{r}\right)e^{-(r/r_0^{\alpha})^2}, \tag{1}$$

and we recalculated the band structure self-consistently. The parameters $\bar{V}^{\alpha}$, V_0^{α}, and r_0^{α} in Eq. (1) were fitted to GaAs experimental energy levels. For empty spheres centered at the interstitial site, $R_{\rm MT}=2.05$ a.u. was used. Table I gives these parameters. These same parameters were then used for $ZnGeAs_2$ by assuming the cations Zn and Ge have the same LDA correction as Ga. Since the average of Zn and Ge is Ga, this assumption is quite reasonable. This procedure provides a more realistic correction to the LDA band-gap error than shifting the conduction bands rigidly upward, because the correction depends on the k point in our procedure. Note that this procedure was done only for the band-structure calculation; no corrections were used for the total-energy calculation.

TABLE I. Fitted parameters $\bar{V}$, V_0, and r_0 for As, Ga, Zn, Ge, empty spheres $(ES)_{As}$ (next to As site), and $(ES)_{cation}$ (next to the cation site) for the LDA corrections [see Eq. (1)].

Atom	$\bar{V}$ (Ry)	V_0 (Ry)	r_0 (a.u.)
As	0.0	120	0.025
Zn, Ga, Ge	0.0	270	0.025
$(ES)_{As}$	0.40	100	0.025
$(ES)_{cation}$	0.24	100	0.025

The valence-band offset was obtained using a procedure similar to that used in core-level photoemission measurements.[14,15] In this procedure,

$$\Delta E_v=\Delta E_{{\rm VBM},c}^{ZnGeAs_2}-\Delta E_{{\rm VBM},c'}^{GaAs}-\Delta E_{\rm core}, \tag{2}$$

where $\Delta E_{{\rm VBM},c}^{ZnGeAs_2}$ and $\Delta E_{{\rm VBM},c'}^{GaAs}$ are the core-level binding energy [relative to the valence-band maximum (VBM)] for $ZnGeAs_2$ and GaAs, respectively, and $\Delta E_{\rm core}$ is the core-level difference $E_c^{ZnGeAs_2}-E_{c'}^{GaAs}$, which is obtained from the calculation for the $(ZnGeAs_2)_n(GaAs)_{2n}$ superlattices with (001) orientation. The superlattice layer thickness n was increased until the core levels of the innermost layer on each side of the superlattice become bulklike. In this study, we used $n=4$. The uncertainty in our calculated ΔE_v was about 0.02 eV. The conduction-band offset was obtained using the relation $\Delta E_c=\Delta E_g-\Delta E_v$, where ΔE_g is the band-gap difference between GaAs and $ZnGeAs_2$. We used the value from our LDA-corrected calculations.

III. RESULTS

In the following, we discuss the significant physics of our calculated results.

A. Structural parameters of $ZnGeAs_2$

Table II gives our LDA-calculated equilibrium structural parameters for both $ZnGeAs_2$ and GaAs (for comparison). The LDA results are also compared with available experimental data.[12]

For $ZnGeAs_2$, the calculated parameters $c/2a=0.988$ and $u=0.249$ are close to the ideal values of $c/2a=1.0$ and $u=0.25$. In the chalcopyrite structure, the difference between the bond lengths $R_{\rm Zn\text{-}As}$ and $R_{\rm Ge\text{-}As}$ is given by

$$R_{\rm Zn\text{-}As}-R_{\rm Ge\text{-}As}=\frac{(u-0.25)a^2}{R_{\rm Zn\text{-}As}+R_{\rm Ge\text{-}As}}. \tag{3}$$

Therefore, the fact that we find the u parameter to be close to 0.25 indicates that the Zn-As bond length is nearly identical to that of the Ge-As bond length, as predicted by Phillips's tetrahedral radii.[24] Because the Zn^{2+} ionic radiius is about 0.12 Å larger than the Ge^{4+} ionic radius,[9,25] our results in-

TABLE II. Calculated equilibrium structural parameters a, c/a, and u, bulk modulus B, calculated low-temperature band gap E_g (with the LDA correction), crystal-field splitting Δ_{CF}, and spin-orbit splitting Δ_0 for chalcopyrite $ZnGeAs_2$. The calculated results are compared with the binary analog GaAs and experimental values at room temperature. (Ref. 12).

	$ZnGeAs_2$		GaAs	
Properties	Calc.	Expt.	Calc.	Expt.
a(Å)	5.6352	5.6712	5.6490	5.6533
$c/2a$	0.988	0.983	1.0	1.0
u	0.249		0.25	0.25
B (Mbar)	0.721		0.742	0.756
E_g^{LDA+C}	1.20	1.15	1.51	1.52 [a]
Δ_{CF}	−0.09	−0.06	0.0	0.0
Δ_0	0.32	0.31	0.34	0.34 [a]

[a]Low-temperature value.

dicate that significant covalent character exists in $ZnGeAs_2$, especially between the Ge-As bond.

Our calculated lattice mismatch between $ZnGeAs_2$ and GaAs is less than 0.2%, in good agreement with experimental data. Our predicted bulk modulus for $ZnGeAs_2$ is $B=0.721$ Mbar, also close to the calculated result of $B=0.743$ Mbar for GaAs. These results indicate that $ZnGeAs_2$ and GaAs have very similar lattice and elastic properties; thus, in an epitaxial growth, the interfacial strain between these two compounds is small.

B. Band structure of $ZnGeAs_2$

Figure 1 plots the fully relativistic (including spin-orbit coupling) electron band structure for $ZnGeAs_2$ and GaAs. The LDA correction is included. We plot the band along two high-symmetry lines T-Γ and Γ-N. The point T is at $(4\pi/c)(0,0,\frac{1}{2})$, and point N is at $(2\pi/a)(\frac{1}{2},\frac{1}{2},0)$. For easy comparison, the zinc-blende GaAs bands are projected on the smaller chalcopyrite Brillouin zone. Table II gives our calculated band-structure parameters for $ZnGeAs_2$ and GaAs. For GaAs, the spin-orbit interaction splits the sixfold top of the valence band into a higher-energy fourfold-degenerate (including spin) Γ_{8v} state and a lower-energy twofold-degenerate Γ_{7v} state. For $ZnGeAs_2$, the noncubic crystal field further splits these states into three twofold-degenerate states Γ_{7v}, Γ_{6v}, and Γ_{7v}. The spin-orbit parameter for $ZnGeAs_2$ was obtained using the quasicubic model.[26]

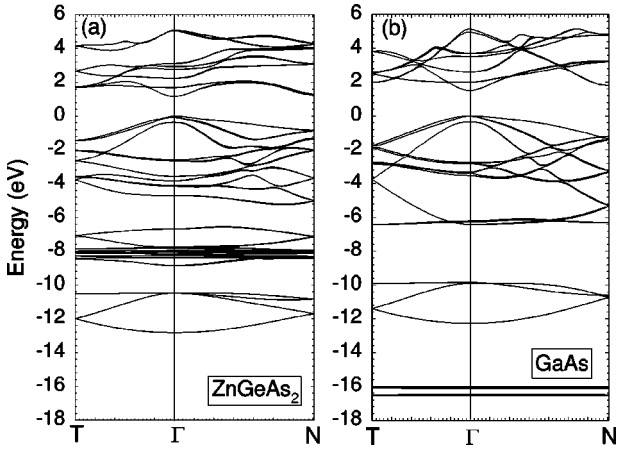

FIG. 1. Calculated LDA-corrected, fully relativistic band structures for (a) $ZnGeAs_2$ and (b) GaAs. The latter is projected to the smaller chalcopyrite Brillouin zone. The VBM is at energy zero. The calculated Zn d bands are at about E_v-8 eV, and the calculated Ga d bands are at about E_v-16 eV. The calculated Ge d bands are at E_v-25 eV (not shown).

For GaAs, the calculated spin-orbit splitting is $\Delta_0=0.34$ eV, in perfect agreement with the experimental value of 0.34 eV.[12] For $ZnGeAs_2$, the calculated spin-orbit splitting $\Delta_0=0.32$ eV is also in good agreement with the experimental[12] value of 0.31 eV. That Δ_0 for $ZnGeAs_2$ is smaller than the value for GaAs can be traced to the larger amount of Zn $3d$ orbital at the VBM of $ZnGeAs_2$ relative to the Ga $3d$ orbital at the VBM of GaAs. Because the d orbital has a negative contribution to the spin-orbit splitting,[27] the large amount of d orbital in the VBM will reduce the value of Δ_0. The calculated crystal-field splitting $\Delta_{CF}=\Gamma_{5v}-\Gamma_{4v}$ for $ZnGeAs_2$ is negative (it is exactly zero for GaAs). This is consistent with the fact that the strain $\epsilon=c/2a-1$ is negative for $ZnGeAs_2$; thus, the [001] epitaxial deformation potential moves the energy of the Γ_{4v} state above the energy of the Γ_{5v} state.[28]

The calculated band structures depicted in Fig. 1 show that, similar to GaAs, $ZnGeAs_2$ in the chalcopyrite structure has a direct Γ-Γ band gap of 1.20 eV at low temperature. This result can be compared with experimentally observed *room-temperature* band gaps of 0.8 to 1.15 eV.[6–8,12] Our result indicates that the small band gap of ~0.8 eV reported by Vaipolin *et al.*[6] and Sobolev and Donetskikh[7] is not the one for $ZnGeAs_2$ at the ground-state structure. It is possible that this low-energy transition is due to defects or imperfections of the crystal (see below).

C. $ZnGeAs_2$ in other ordered structures

It is interesting to compare the properties of $ZnGeAs_2$ in the chalcopyrite structure with the properties of $ZnGeAs_2$ in other small-unit-cell ordered structures, which have been observed in other chalcopyrite compounds.[29] Our results for $ZnGeAs_2$ in the chalcopyrite structure, CuAu structure (a Zn/Ge superlattice along the [001] direction), and CuPt structure (a Zn/Ge superlattice along the [111] direction) are summarized in Table III. We see that (i) $ZnGeAs_2$ in the chalcopyrite structure is indeed the ground-state structure. The formation energy of $ZnGeAs_2$ in the chalcopyrite structure is much lower than the formation energy of $ZnGeAs_2$ in the CuAu or CuPt structures, even though in the CuAu structure As has the same local Zn_2Ge_2 tetrahedral nearest neighbors around it; (ii) the band gap of $ZnGeAs_2$ also depends sensitively on the cation atomic arrangements. A large band-gap reduction is expected for $ZnGeAs_2$ if the cation distribution deviates from the chalcopyrite structures. Because the cation distribution in chalcopyrite compounds depends strongly on the growth temperature,[13] the strong correlation of the band gap to the cation distribuition for $ZnGeAs_2$ pro-

TABLE III. Calculated formation energy differences $E_f(\sigma) - E_f$(chalcopyrite) and band-gap reduction $E_g(\sigma) - E_g$(chalcopyrite) ($\sigma =$ CuAu and CuPt) for $ZnGeAs_2$ and $CuGaSe_2$.

Compounds	CuAu	CuPt
Formation-energy difference (in meV/atom)		
$ZnGeAs_2$	23	56
$CuGaSe_2$	9	63
Band-gap reduction (in eV)		
$ZnGeAs_2$	−0.62	−1.71
$CuGaSe_2$	−0.23	−1.32

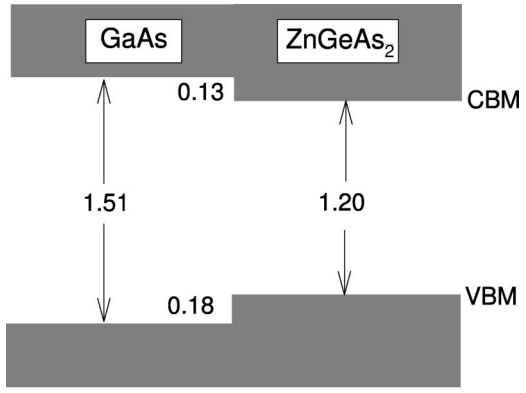

FIG. 2. Schematic plot of the calculated band offset at the $ZnGeAs_2$/GaAs interface. Energies are in eV.

vides an opportunity for band-gap engineering by controlling temperature and other growth conditions.

For comparison, we compared our results for $ZnGeAs_2$ with those for $CuGaSe_2$ (Table III). First, we find that the formation energy difference ΔE_f(CuAu) is much larger for $ZnGeAs_2$ than that for $CuGaSe_2$. Because the CuAu and chalcopyrite structures have the same fcc nearest-neighbor local environment but different second-neighbor environments, ΔE_f(CuAu) is determined mostly by the bond-bending force. Because $ZnGeAs_2$ is more covalent than $CuGaSe_2$, $ZnGeAs_2$ has a larger bond bending force constant and hence a larger ΔE_f(CuAu). On the other hand, ΔE_f(CuPt) for $ZnGeAs_2$ is determined mostly by the deviation from the octet rule,[13] i.e., in the CuPt structure, the average charge of the cation tetrahedron around each As is either 2.5 (for the Zn_3Ge cluster) or 3.5 (for the $ZnGe_3$ cluster), but not 3. This effect is found to be larger for $CuGaSe_2$ than for $ZnGeAs_2$. Second, we find that the band-gap reduction in $ZnGeAs_2$ is much larger than that in $CuGaSe_2$. The band-gap reduction in the CuAu and CuPt structures is mainly due to band-folding-induced intraband coupling in the conduction band (Γ-X for the CuAu structure and Γ-L for the CuPt structure).[30] In perturbation theory, the downward shift of the conduction-band minimum (CBM) energy is inversely proportional to the energy difference of the coupled states. Because $ZnGeAs_2$(GaAs) is more covalent than $CuGaSe_2$(ZnSe), the energy differences between the zinc-blende Γ_{1c}- and X_{3c}-derived states and between zinc-blende Γ_{1c}-and L_{1c}-derived states are smaller in $ZnGeAs_2$(GaAs) than in $CuGaSe_2$(ZnSe); thus, the band-gap reduction in $ZnGeAs_2$ is larger than that in $CuGaSe_2$.

D. $ZnGeAs_2$/GaAs band alignment

The calculated band gap for $ZnGeAs_2$ in the chalcopyrite structure is about 0.31 eV smaller than the band gap of GaAs. To study the origin of this band-gap narrowing, we have calculated the band alignment between $ZnGeAs_2$ and GaAs using the procedure described in Sec. II. The calculated results are show in Fig. 2. Our results show that the band-gap narrowing of $ZnGeAs_2$ relative to its binary analog GaAs is due to the (a) decrease of its conduction-band minimum (CBM) by 0.13 eV, and (b) increase of the $ZnGeAs_2$ VBM by 0.18 eV. To understand these energy shifts, we plotted in Fig. 3 the CBM and VBM electron charge densities in the $(1\bar{1}0)$ plane for both $ZnGeAs_2$ and GaAs. We find the following. (a) By symmetry, the CBM consists of antibonding cation s and anion s characters. When Ga+Ga is transmuted into Zn+Ge, more electrons are localized on Ge than on Zn [see Fig. 3(a)], because the Ge 4s states are deeper in energy than the Ga 4s and Zn 4s states. The localization of the CBM on the Ge site shifts the $ZnGeAs_2$ CBM downward and thus explains the band alignment ΔE_c. (b) On the other hand, by symmetry, the VBM state in zinc-blende and chalcopyrite structures consists primarily of the anion p character coupled with some cation p and d states. For a common-anion system, the valence-band offset is dominated by the anion p and cation d couplings, because the cation p orbital energies are very similar.[27] For the system studied here, the cation d bands are below the anion p bands; thus, VBM is an anion p and cation d antibonding state, as shown in Fig. 3. By perturbation theory,[32] the upward shift of the VBM due to the p-d repulsion is given by $V_{pd}^2/\Delta E_{pd}$, where ΔE_{pd} is the energy separation between the anion p state and the cation d state, and V_{pd}^2 is the square of the coupling matrix. Because the upward shift of the VBM is inversely proportional to ΔE_{pd}, the higher the cation d or-

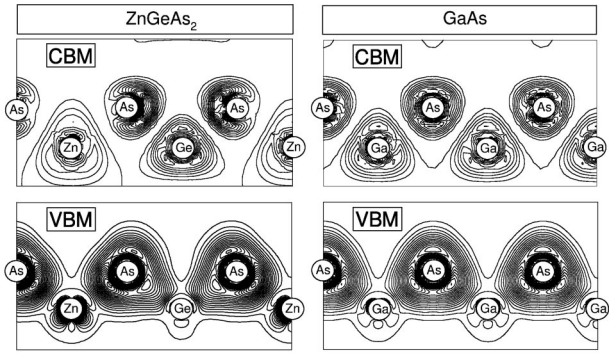

FIG. 3. Contour plot of electronic charge density of valence-band maximum (VBM) and conduction-band minimum (CBM) states for $ZnGeAs_2$ and GaAs in the $(1\bar{1}0)$ plane.

bital energy is, the larger the p-d repulsion will be, which leads to a higher VBM. In Fig. 1, we show that the Zn $3d$ band is much shallower than the Ga $3d$ band, which is higher in energy than Ge $3d$ (not shown in the figure). Thus, the p-d coupling is much larger between Zn and As. Indeed, Fig. 3 shows that a large Zn $3d$ antibonding character is present at the VBM of $ZnGeAs_2$. To see the trend of the VBM energy shift more quantitatively, we assume that ΔE_{pd} decreases linearly as a function of the $3d$ cation atomic number[31] and that V_{pd}^2 is independent of the cation. Under these assumptions and using perturbation theory,[32] we can show that the p-d coupling contribution to the ΔE_v is given by

$$\frac{2V_{pd}^2}{\Delta E_{pd}(\mathrm{GaAs})}\,\frac{\delta_{dd}^2}{\Delta E_{pd}^2(\mathrm{GaAs})-\delta_{dd}^2}. \tag{4}$$

Here, δ_{dd} is the d orbital energy difference between Zn and Ga $3d$ states or between Ga and Ge $3d$ states. Equation (4) explains why $ZnGeAs_2$ has a higher VBM than GaAs. Equation (4) also shows that the effect of the p-d repulsion on the valence-band offset will be larger if ΔE_{pd} of the binary analog is small. This is the case for the ZnSe/$CuGaSe_2$ system. Because $\Delta E_{pd}(\mathrm{ZnSe})\approx 7$ eV is much smaller than $\Delta E_{pd}(\mathrm{GaAs})\approx 16$ eV, the valence-band offset[15] $\Delta E_v = 0.66$ eV between ZnSe and $CuGaSe_2$ is much larger than the value $\Delta E_v = 0.18$ eV that we find here between GaAs and $ZnGeAs_2$. The large valence-band offset between ZnSe and $CuGaSe_2$ also leads to a larger band-gap reduction (0.99 eV) between ZnSe and $CuGaSe_2$ than the band-gap reduction found here (0.31 eV) between GaAs and $ZnGeAs_2$.

E. Stability and electronic structure of $(ZnGeAs_2)_{1-x}(GaAs)_{2x}$ alloys

To form heterojunction devices using $ZnGeAs_2$ and GaAs, it is important to know the formation energies of $(ZnGeAs_2)_{1-x}(GaAs)_{2x}$ alloys and $(ZnGeAs_2)_n(GaAs)_{2n}$ superlattices, as well as the wave-function localization in different sublattices. We have calculated first the formation energy of $(ZnGeAs_2)_{0.5}(GaAs)$ in the ordered stannite structure, which is a ZnAs/GaAs/GeAs/GaAs superlattice stacked along the [201] direction. The calculated formation enthalpy,

$$\Delta H(x=\tfrac{1}{2}) = E_{\mathrm{tot}}(\tfrac{1}{2}) - \tfrac{1}{2}E_{\mathrm{tot}}(\mathrm{ZnGeAs_2}) - E_{\mathrm{tot}}(\mathrm{GaAs}), \tag{5}$$

is found to be very small, with $\Delta H(x=\frac{1}{2}) = 2.6$ meV/cation, indicating that at low temperature, the $(ZnGeAs_2)_{0.5}(GaAs)$ alloy will form long-range ordered $ZnGeGa_2As_4$ in the stannite structure. The very small formation energy found in this system is related to the fact that $ZnGeAs_2$ and GaAs are nearly lattice matched.

The calculated bowing parameter b for the direct band gap of $(ZnGeAs_2)_{1-x}(GaAs)_{2x}$ can be obtained by fitting the calculated band gap to the quadratic equation

$$E_g(x) = (1-x)E_g(\mathrm{ZnGeAs_2}) + xE_g(\mathrm{GaAs}) - bx(1-x). \tag{6}$$

TABLE IV. Calculated formation energies ΔH_n (in meV/atom) and bowing parameters b_n (in eV) of $(ZnGeAs_2)_n(GaAs)_{2n}$ superlattices along the [001] direction as a function of layer thickness n.

n	ΔH_n	b_n
1	1.3	0.04
2	9.2	0.97
4	3.5	0.29

In the stannite structure, it is also very small, with $b = 0.04$ eV. However, because the formation energy and the band gap of $ZnGeAs_2$ depend sensitively on the cation distribution, the formation energy and the band gap of the $(ZnGeAs_2)_{1-x}(GaAs)_{2x}$ alloy are also expected to depend sensitively on the cation distribution, which is determined by growth conditions.

F. Stability and electronic structure of $(ZnGeAs_2)_n(GaAs)_{2n}$ superlattices

We have also studied the stabilities of the $(ZnGeAs_2)_n(GaAs)_{2n}$ superlattices along the [001] direction as a function of layer thickness n. The superlattices are formed by replacing alternating n $ZnGeAs_2$ layers by n $(GaAs)_2$ layers. The results are shown in Table IV. We find that at $n=1$, which is equivalent to the stannite structure, the formation energy $\Delta H_{n=1}$ is nearly zero. The formation energy per atom reaches its maximum value at $n=2$ and goes to zero at large n because the two constituents are lattice matched. To investigate the nonmonotonic behavior of ΔH_n, we have calculated the Madelung energy contribution to the superlattice formation energy ΔH_n^M. We assigned the nominal charge to each atom, that is, $+2$, $+3$, $+4$, and -3 for Zn, Ga, Ge, and As, respectively. We find that the ΔH_n^M follow the same trend as the total superlattice formation energies, i.e., $\Delta H_{n=1}^M = \Delta H_{n=\infty}^M = 0$, and ΔH_n^M reach their maximum value at $n=2$. This indicates that for this lattice-matched system, the superlattice formation energy is dominated by the Coulomb interaction.

The smallness of ΔH_n for $n=1$ suggests that it is difficult to form a sharp $(ZnGeAs_2)_n(GaAs)_{2n}$ superlattice with $n>1$ because the thick superlattice is unstable with respect to the $n=1$ superlattice; thus, interlayer atomic exchange between the Ga atoms and (Zn,Ge) atoms at the superlattice will occur. Further experimental study is needed to test our predictions.

Table IV also shows the band-gap bowing parameters b_n as a function of the superlattice thickness n. We find that, similar to the superlattice formation energy, the band-gap bowing is nonmonotonic, with a large band-gap bowing at $n=2$. Similar nonmonotonic behavior of band-gap oscillations has been observed and explained in zinc-blende-based semiconductor polytypes.[33]

Figure 4 plots the electron charge density of the VBM states and the CBM state for the $(ZnGeAs_2)_4(GaAs)_8$ superlattice in the $(1\bar{1}0)$ plane. Figure 5 shows the corresponding plane-averaged charge densities $\rho(z) = \int \rho(x,y,z)\,dx\,dy$

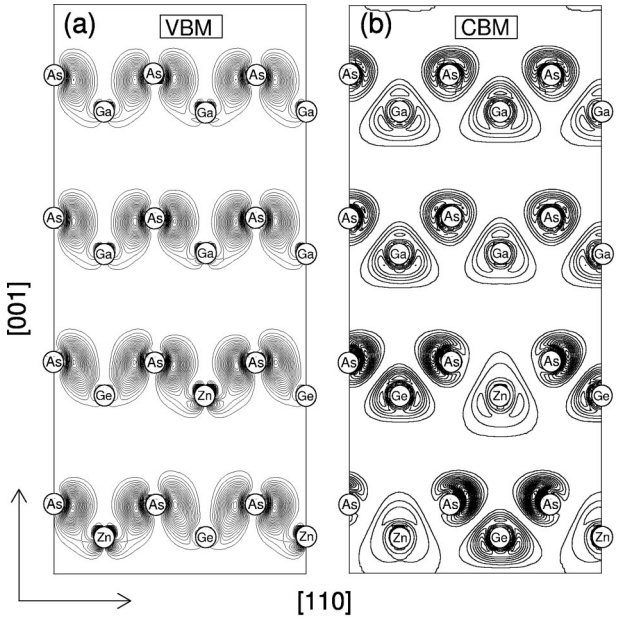

FIG. 4. Contour plot of electronic charge densities of (a) valence-band maximum (VBM) and (b) conduction-band minimum (CBM) states for the superstructure $(ZnGeAs_2)_2/(GaAs)_4$ in the $(1\bar{1}0)$ plane.

along the $z=[001]$ direction. We also plotted the cell-averaged charge density $\overline{\rho}(z)=\int_{-c/2}^{c/2}\rho(z)dz$, where c is the period along the z direction. We see that both the CBM and VBM are slightly more localized on the $ZnGeAs_2$ side. This result is consistent with our band-alignment calculation (Fig. 3), which shows that the $ZnGeAs_2$/GaAs system has a type-I band alignment, with both holes and electrons localized on $ZnGeAs_2$.

IV. SUMMARY

In summary, we systematically studied the electronic and structural properties of $ZnGeAs_2$/GaAs systems through first-principles band-structure calculations. We find the following. (a) In agreement with experimental data, $ZnGeAs_2$ is nearly lattice matched to its binary analog GaAs. (b) $ZnGeAs_2$ has a direct band gap, about 0.31 eV smaller than the band gap of GaAs. (c) At $x=0.5$, the $(ZnGeAs_2)_{1-x}(GaAs)_{2x}$ alloy forms a stable stannite structure. The calculated alloy optical bowing parameter for the stannite structure $b=0.04$ eV is very small. (d) The calculated valence-band offset and conduction-band offset between $ZnGeAs_2$ and GaAs are 0.18 eV and 0.13 eV, respectively, with both holes and electrons localized on $ZnGeAs_2$ (i.e., the alignment is type I). (e) The formation energy of the $(ZnGeAs_2)_{n/2}(GaAs)_n$ superlattice is nonmonotonic, indicating that it will be difficult to form sharp $ZnGeAs_2$/GaAs interfaces. Our calculated results for the $ZnGeAs_2$/GaAs system are compared with the $CuGaSe_2$/ZnSe system. We show that, relative to the $CuGaSe_2$/ZnSe system, the band-gap reduction and valence-band offset between $ZnGeAs_2$ and GaAs are small. The differences between $ZnGeAs_2$/GaAs and $CuGaSe_2$/ZnSe are explained in terms of the ionicity and the relative strength of the p-d coupling in these two systems.

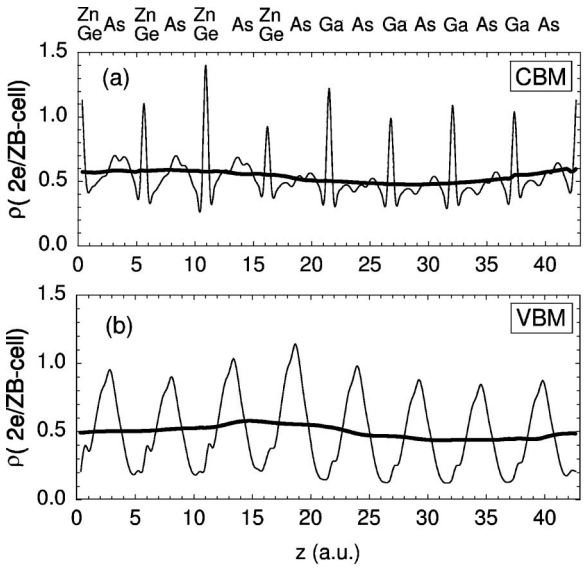

FIG. 5. The plane-averaged charge densities $\rho(z)$ (solid thin line), and the z-averaged charge density $\overline{\rho}(z)$ (solid thick line), along the $z=[001]$ direction. Note that both the CBM and VBM states are more localized on the $ZnGeAs_2$ side.

ACKNOWLEDGMENTS

This work was funded under the Dual Use Science and Technology (DUS & T) program by the Air Force Research Laboratory, Space Vehicles Directorate (AFRL/VS), and by Hughes Spectrolab. The work was completed at the National Renewable Energy Laboratory under the DOE Contract No. DE-AC36-99GO10337.

[1] J. L. Shay and J. H. Wernick, *Ternary Chalcopyrite Semiconductors: Growth, Electronic Properties and Applications* (Pergamon, Oxford, 1974).

[2] J.E. Jaffe and Alex Zunger, Phys. Rev. B **27**, 5176 (1983); *ibid.* **29**, 1882 (1984); *ibid.* **30**, 741 (1984).

[3] C.K. Sinclair, in *Proceedings of the 8th International Symposium on High Energy Spin Physics*, edited by K. J. Heller, AIP Conf. Proc. (AIP, New York, 1989), p. 1412.

[4] S.-H. Wei, in *Proceedings of the 7th International Workshop on Polarized Gas Targets and Polarized Beams*, edited by R. J. Holt and M. A. Miller AIP Conf. Proc. (AIP, New York, 1998), p. 284.

[5] Sarah R. Kurtz, D. Myers, and J. M. Olsen, in *Proceedings 26th IEEE Photovoltaics Specialist Conference* (IEEE, New York, 1997), p. 875.

[6] A.A. Vaipolin, N.A. Goryunova, E.O. Osmanov, Yu.V. Rud, and

D.N. Tretyakov, Dokl. Akad. Nauk SSSR **154**, 1116 (1964).
[7] V.V. Sobolev and V.I. Donetskikh, Fiz. Tverd. Tela (Leningrad) **12**, 2716 (1970).
[8] G.S. Solomon, M.L. Timmons, and J.B. Posthill, J. Appl. Phys. **65**, 1952 (1989).
[9] L. Pauling, *The Nature of the Chemical Bond* (Cornell University Press, Ithaca, New York, 1967).
[10] A.A. Vaipolin, Fiz. Tverd. Tela (Leningrad) **15**, 1430 (1973).
[11] M. Levalois and G. Allais, Phys. Status Solidi A **109**, 111 (1988).
[12] *Semiconductors—Basic Data*, edited by O. Madelung (Springer-Verlag, New York, 1996).
[13] S.-H. Wei, L.G. Ferreira, and A. Zunger, Phys. Rev. B **45**, 2533 (1992).
[14] S.-H. Wei and A. Zunger, Appl. Phys. Lett. **63**, 2549 (1993).
[15] S.-H. Wei and A. Zunger, J. Appl. Phys. **78**, 3846 (1995).
[16] S.-H. Wei, A. Zunger, I.-H. Choi, and P.Y. Yu, Phys. Rev. B **58**, R1710 (1998).
[17] P. Hohenberg and W. Kohn, Phys. Rev. **136**, B864 (1964); W. Kohn and L.J. Sham, *ibid.* **140**, A1133 (1965).
[18] S.-H. Wei and H. Krakauer, Phys. Rev. Lett. **55**, 1200 (1985), and references therein.
[19] D.M. Ceperley and J.B. Alder, Phys. Rev. Lett. **45**, 566 (1980).
[20] J. Perdew and A. Zunger, Phys. Rev. B **23**, 5048 (1981).
[21] H.J. Monkhorst and J.P. Pack, Phys. Rev. B **13**, 5188 (1976).
[22] S. Froyen, Phys. Rev. B **39**, 3168 (1989).
[23] N.E. Christensen, Phys. Rev. B **30**, 5753 (1984).
[24] J. C. Phillips, *Bonds and Bands in Semiconductors* (Academic, New York, 1973).
[25] R.D. Shannon, Acta Crystallogr., Sect. A: Cryst. Phys., Diffr., Theor. Gen. Crystallogr. **32**, 751 (1976).
[26] J.J. Hopfield, J. Phys. Chem. Solids **15**, 97 (1960).
[27] S.-H. Wei and A. Zunger, Phys. Rev. B **37**, 8958 (1988).
[28] S.-H. Wei and A. Zunger, Phys. Rev. B **49**, 14 337 (1994).
[29] D.S. Su and S.-H. Wei, Appl. Phys. Lett. **74**, 2483 (1999).
[30] S.-H. Wei and A. Zunger, Phys. Rev. B **39**, 3279 (1989).
[31] S.-H. Wei and A. Zunger, Phys. Rev. B **60**, 5404 (1999).
[32] S.-H. Wei and A. Zunger, Phys. Rev. Lett. **59**, 144 (1987).
[33] S.-H. Wei, S.B. Zhang, and A. Zunger, Phys. Rev. B **59**, R2478 (1999).